Elevated Wnt2 and Wnt4 activate NF-κB signaling to promote cardiac fibrosis by cooperation of Fzd4/2 and LRP6 following myocardial infarction

Chao Yin[a,1], Zhishuai Ye[b,1], Jian Wu[a,1], Chenxing Huang[a], Le Pan[a], Huaiyu Ding[c], Lei Zhong[c], Lei Guo[c], Yan Zou[a], Xiang Wang[a], Ying Wang[a], Pan Gao[a], Xuejuan Jin[a], Xiaoxiang Yan[d], Yunzeng Zou[a], Rongchong Huang[b,*], Hui Gong[a,*]

[a] NHC Key Laboratory of Viral Heart Diseases, Shanghai Institute of Cardiovascular Diseases, Zhongshan Hospital, and Institutes of Biomedical Sciences, Fudan University, Shanghai 200032, China
[b] Department of Cardiology, Beijing Friendship Hospital, Capital Medical University, Beijing 100053, China
[c] Department of Cardiology, The First Affiliated Hospital of Dalian Medical University, Dalian 116011, China
[d] Department of Vascular and Cardiology, Ruijin Hospital, Shanghai Jiao Tong University School of Medicine, Shanghai, China

ARTICLE INFO

ABSTRACT

Background: Acute myocardial infarction (AMI)-induced excessive myocardial fibrosis exaggerates cardiac dysfunction. However, serum Wnt2 or Wnt4 level in AMI patients, and the roles in cardiac fibrosis are largely unkown.
Methods: AMI and non-AMI patients were enrolled to examine serum Wnt2 and Wnt4 levels by ELISA analysis. The AMI patients were followed-up for one year. MI mouse model was built by ligation of left anterior descending branch (LAD).
Findings: Serum Wnt2 or Wnt4 level was increased in patients with AMI, and the elevated Wnt2 and Wnt4 were correlated to adverse outcome of these patients. Knockdown of Wnt2 and Wnt4 significantly attenuated myocardial remodeling and cardiac dysfunction following experimental MI. *In vitro,* hypoxia enhanced the secretion and expression of Wnt2 and Wnt4 in neonatal rat cardiac myocytes (NRCMs) or fibroblasts (NRCFs). Mechanistically, the elevated Wnt2 or Wnt4 activated β-catenin /NF-κB signaling to promote pro-fibrotic effects in cultured NRCFs. In addition, Wnt2 or Wnt4 upregulated the expression of these Wnt co-receptors, frizzled (Fzd) 2, Fzd4 and (ow-density lipoprotein receptor-related protein 6 (LRP6). Further analysis revealed that Wnt2 or Wnt4 activated β-catenin /NF-κB by the co-operation of Fzd4 or Fzd2 and LRP6 signaling, respectively.
Interpretation: Elevated Wnt2 and Wnt4 activate β-catenin/NF-κB signaling to promote cardiac fibrosis by cooperation of Fzd4/2 and LRP6 in fibroblasts, which contributes to adverse outcome of patients with AMI, suggesting that systemic inhibition of Wnt2 and Wnt4 may improve cardiac dysfunction after MI.

1. Introduction

Acute myocardial infarction (AMI), a severe cardiovascular disease, remains a leading cause of death worldwide [1]. Although percutaneous coronary intervention (PCI) technology application has significantly decreased mortality of patients with AMI, a considerable number of patients still undergo excessive cardiac fibrosis or ventricular remodeling after infarction, which eventually leads to cardiac dysfunction [2,3]. At the acute phase of MI, cardiac fibrosis in infarcted area can effectively prevent left ventricular rupture. However, excessive myocardial fibrosis during the chronic stage of MI reduces ventricular compliance, leading to systolic and diastolic dysfunction and arrhythmia [3,4]. Therefore, inhibition of excessive fibrosis is very meaningful for improving the cardiac function and prognosis of patients with MI.

MI, Myocardial infarction; Fzd, Frizzled
* Corresponding authors.
E-mail addresses: rchuang@ccmu.edu.cn (R. Huang), gonghui2005@fudan.edu.cn (H. Gong).
[1] These authors contributed equally to this work.

Research in context

Evidence before this study

Excessive cardiac fibrosis in response to myocardial infarction (MI) leads to the cardiac dysfunction. The mRNAs of Wnt ligands, including Wnt2 and Wnt4, have been shown to be a strong upregulation in heart tissue following experimental MI. Wnt2 or Wnt4 promotes smooth muscle cell proliferation and migration. However, serum Wnt2 or Wnt4 level in AMI patients, and the roles in cardiac fibrosis are not fully understood.

Added value of this study

We found serum Wnt2 and Wnt4 both increased in patients with AMI, and the high serum Wnt2 and Wnt4 levels were correlated to adverse outcome of these patients. Knockdown of Wnt2 and Wnt4 significantly attenuated myocardial fibrosis, reduced infarct area and improved cardiac dysfunction after experimental MI. Inhibition of β-catenin/NF-κB signaling, knockdown of Fzd4/2 or LRP6 signaling greatly reversed the pro-fibrotic effects of Wnt2 or Wnt4 in cardiac fibroblasts.

Implications of all the available evidence

Increased serum Wnt2 or Wnt4 level significantly contributed to cardiac fibrosis following MI. Inhibition of Wnt2 and Wnt4 signaling may have a great therapeutic potential following MI by limiting excessive cardiac fibrosis.

The Wnt protein family, a class of highly conserved secreted proteins rich in cysteine [5], is expressed in various tissues and cells. Wnt ligands activate membrane receptors, the Frizzled (Fzd) family, and lipoprotein receptor-related protein (LRP)-5/6 or other co-receptors, to regulate multiple pathophysiological processes including cell apoptosis, proliferation and differentiation [5,6]. The Wnt signaling pathway has been mainly divided into: (1) the canonical Wnt/β-catenin signaling, (2) the non-canonical Wnt/Ca^{2+} signaling, (3) the Wnt/planar cell polarity signaling [7,8]. A variety of physiological effects of Wnt signaling mainly depend on the activation of different types of receptors [9,10]. In animal study, members of Wnt family, Wnt2, Wnt4, Wnt10b and Wnt11, show a strong upregulation in the transcription levels in heart tissue following experimental MI [11,12]. Wnt10b is increased transiently in peri-infarct cardiomyocytes, which promotes angiogenesis and inhibits cardiac fibrosis [12]. Our preliminary data revealed that serum Wnt2 or Wnt4 but not Wnt11 was increased in patients with AMI. Wnt2 or Wnt4, a member of Wnt protein family, regulates a variety of organ or tissue functions in adult organisms [13]. Wnt2 promotes endothelial and cardiomyocyte differentiation but inhibits hemangioblast differentiation and hematopoiesis in murine embryonic stem cells [14,15]. Moreover, elevated Wnt2 protein level has been observed in mouse models of systemic sclerosis, and inhibition of β-catenin mediates the decreased Wnt2 expression in human keloid fibroblasts [16,17]. During kidney development, Wnt4 is very critical for tubulogenesis [18]. Wnt4 is significantly upregulated [19], and regulates the transition of pericyte cells into myofibroblasts after acute kidney injury [20]. However, whether serum Wnt2 or Wnt4 is increased in patients with AMI, the relationship between high Wnt2 or Wnt4 and poor outcome, and the roles in cardiac fibrosis are largely unknown.

Therefore, we aimed to compare serum Wnt2 and Wnt4 between AMI patients and non-AMI patients, observe one-year follow-up outcome in AMI cohort patients and investigate the potential molecular mechanisms involved cardiac fibrosis by building mouse AMI model.

2. Methods

2.1. Study populations

The Wnt2/Wnt4 human study was performed in the First Affiliated Hospital of Dalian Medical University (Dalian, China). Nested case-control design based on the chest discomfort cohort. Cases were defined as patients with AMI, they were followed up for one-year for the incidence of the adverse outcomes. Patients (aged 45−80, admission within 24 h from chest discomfort) received an angiography examination because of the possible coronary heart disease between May 2018 and November 2018 were enrolled. Diagnoses were based on the "2018 ESC/ ACC/AHA/WHF Guidelines for Fourth universal definition of myocardial infarction (2018)" [21]. Exclusion criteria were: previous MI, severe heart failure, advanced liver or renal diseases, chronic or acute infections, autoimmune diseases, abnormal hematopoietic function, malignancies, and cancer. Using matching (age, sex, hypertension, diabetes), we generated a comparable sample of controls who claimed chest discomfort but had normal coronary arteries on angiography (non-AMI, as control) selected from the same population as the cases. Finally, 109 patients with AMI and 56 patients were included in the current study. Demographic data, medical and social histories, and baseline characteristics were collected from all cases and controls according to standardized protocols.The blood samples were collected at admission, and the serum Wnt2 and Wnt4 level was detected.

Incident major adverse cardiovascular events (MACEs) were ascertained in AMI patients during one year follow-up. MACEs was defined as re-admission for unstable angina or MI, heart failure, stroke and all cause death. The identification of a MACEs was supported by an annual telephone follow-up and a re-examination in the clinic. All the enrolled AMI patients finished one-year follow-up.

2.2. Ethics

The human study was approved by the Ethics Committee of Dalian Medical University/ First Affiliated Hospital of Dalian Medical University (PJ-KS-KY-2017-104(x)) and registered in www.clinicaltrials.gov (ClinicalTrials.gov Identifier: NCT03342131). Before inclusion in the study, written informed consent was obtained from the patient's family/patient. The investigation conformed to the principles outlined in the Declaration of Helsinki.

All experiment protocols about animal in this study were approved by the Animal Care and Use Committee of Zhongshan Hospital, Fudan University (APP-D-20170325), and conformed to the 'Guidelines for the Care and Use of Laboratory Animals' published by the National Institutes of Health (No. 85−23, revised 1996).

2.3. Baseline Wnt2 and Wnt4 measurements

Serum levels of Wnt2 and Wnt4 were detected by enzyme-linked immunosorbent assay (ELISA). Human Wnt2 and Wnt4 ELISA kits were purchased from CUSABIO company (Cat#: CSB-EL026133HU, CSB-EL026137HU, Wuhan, China) and used following the manufacturer's instructions.

2.4. Animals and myocardial infarction model

C57BL/6 male mice (8−10 weeks, Charles River Laboratories) were used to build MI model. The model was built by permanent coronary artery occlusion as described in a previous study [22]. In brief, the left anterior descending branch (LAD) of mouse was ligated with a 6-0 silk thread, after anaesthesia. The sham operation group received the same surgical operation, except for ligation of LAD. The detailed procedure was described in supplementary methods.

2.5. Echocardiography analysis and hemodynamic measurements

Echocardiography measurement was performed in mice after MI or sham operation. After being anesthetized with 1% isoflurane, the mice were transferred from the anesthesia tank to a heating pad, and then were fixed and changed to mask anesthesia. The function and structure of left ventricle was assessed by the RMV 2100 scan head of Vevo 2100 (VisualSonics Inc.,Canada). Heart rate was maintained above 400 bpm.

The 1.4F cardiac catheter (Millar Instruments, USA) was used to record hemodynamic parameters of mice. After anesthetizing the mice, we inserted the micro-nanometer catheter into the right common carotid artery and introduced into the left ventricle. LV end-diastolic pressure (EDP), dp/dt, -dp/dt and Tau were measured by Power Laboratory system (AD Instruments, Australia).

2.6. ShRNA-adeno-associated virus 9 (AAV9) production and animal injection

ShWnt2/4-AAV9 was synthetized and injected into mice of 8-week-old by tail vein to silence the cardiac Wnt2 and Wnt4 level. ShRNA sequences of mouse Wnt2 and Wnt4 were subcloned into GV478 plasmid to produce AAV9 particles (Hanheng Biotechnology Co, Shanghai, China). Sh-Scramble-AAV9 was generated as a control. ShWnt2 sequence: GGCGTTGTATTTGCCATCATGATGGCAAATACAA-CGCC; shWnt4 sequence: GCACAGTTCAAGCCACATATATGTGGCTT-GAACTGTGC. At 3 weeks before sham or MI surgery, mice were injected with the AAV9 viruses 1.5×10^{12} particles by tail vein.

2.7. Histological staining

The paraffin-embedded heart samples were cut into 5 um thickness sections with Leica slicer and then stained with Masson's trichrome. The images of cardiac fibrosis were pictured by ImageProPlus 6.0 (Media Cybernetics, Rockville, USA). Infarcted area was analyzed using software-Image J (National Institutes of Health, Bethesda, USA).

2.8. Culture of primary neonatal rat cardiomyocytes(NRCMs) and cardiac fibroblasts(NRCFs) and hypoxia model in vitro

We isolated and cultured primary NRCMs and NRCFs from Sprague−Dawley (SD) rats of 1-2 days old with 0.125% trypsin digestion. The detailed method was showed in Supplementary methods. NRCMs or NRCFs were cultured in serum-free DMEM and incubated in a hypoxic incubator (5% CO_2, 94% N_2 and 1% O_2) for different time-points. Cells were cultured in a 21% O_2 incubator as control.

2.9. Isolation of cardiomyocytes and fibroblasts from adult mouse

Cardiomyocytes and fibroblasts of adult mouse were isolated as described in a previous study [23]. The detailed method was showed in Supplementary method.

2.10. Scratch migration assay

Scratch migration assay was used to evaluate the migratory ability of cardiac fibroblasts. In brief, NRCFs were cultured and reached 80% confluence in 6-well plates. A sterile P200 pipette tip was used to make a one pass scratch area along the drawn straight line in the middle of the six-well plates, and then we washed three times with PBS to remove the non-adherent cells. NRCFs were treated with recombinant human Wnt2 or Wnt4 protein in serum-free DMEM medium. Digital images of scratch area were captured at indicated time-points for analysis by ImagePro Plus6.0 (Media Cybernetics, Rockville, USA).

2.11. Real-time quantitative PCR

Total RNA was extracted from cells or tissues using TRIzol reagent from Invitrogen (Cat#:15596026, Carlsbad, CA) according to the manufacturer's recommendations and was reverse transcribed using Takara RT-PCR kit (Cat#: RR036A, TaKaRa, Japan). SYBR qPCR Master Mix (Cat#: Q711-02, Vazyme, Nanjing) was used in qRT-PCR on Roche LightCycler 480 System. Glyceraldehyde 3-phosphate dehydrogenase (GAPDH) was used as the internal control. The primer sequences produced by Sangon Biotech (Shanghai, China) were validated and used (Table S1).

2.12. SiRNA or shRNA lentivirus transfection

Knockdown or silence of target genes by transfection of siRNA into fibroblasts in vitro. The siRNAs targeted to rat Wnt2, Wnt4, Fzd2 and Fzd4 were synthesized by GenePharma (Shanghai, China), and the efficacy of silence was examined, respectively. SiRNA transfection procedure was showed in Supplementary methods. The preparations of LRP6 lentiviral particles were performed as described in our previous study [24]. Cells were transfected with DMEM containing shScamble or shLRP6 lentivirus for 48 h and then followed by PBS, human recombinant Wnt2 (20 ng/ml) or Wnt4(50 ng/ml) in DMEM for another 24 h.`

2.13. Western blot analysis

Tissues or cells were lysed with radioimmunoprecipitation (RIPA) buffer with 1% phenylmethanesulfonyl fluoride (PMSF). The protein concentration was quantified by Bradford Protein Assay Kit (Cat#: 500-0202, Bio-rad, CA). The protein samples of equal amount were loaded onto SDS/PAGE (10%) gels, electrophoresed and then transferred onto polyvinylidene fluoride (PVDF) membranes (Cat#: IPFL00010, Millipore, USA). To block the non-specific signaling, the PVDF membranes were incubated in 5% skimmed milk for 1 h at room temperature. According to the maker, the target-protein blots were chosen and incubated with different primary antibodies overnight (4 °C). Finally, the bands were interacted with an Omni-ECL™Femto Chemiluminescence Kit (Cat#: F03, Willget, Shanghai) and detected by Las-4000 mini imaging system (FUJIFILM Inc, Japan). All the antibodies were validated and used in Table S2.

2.14. Statistical analysis

We calculated that a sample of 156 AMI patients (cases: controls=104:52) and 93 AMI patients (cases: controls=62:31) would provide the trial with 80% power to detect a difference of 0.48 points in the mean Wnt2 and Wnt4 level, respectively, assuming a standard deviation of 1.0 and a significance level of 0.05. The target sample size was determined by Wnt2. For patients with or without AMI, normally distributed variables were expressed as mean ± Standard Deviation (SD), and skewed variables were expressed as median [interquartile range]. To compare the differences between two groups with normally distributed variables, Student's *t* test was used. To test for differences between two groups with skewed variables, the nonparametric Mann-Whitney U test was used. For comparison for more than two groups, one-way analysis of variance (ANOVA) was performed for normally distributed variables, while Kruskal-Wallis test was applied for skewed variables. If the results showed a significant difference, pairwise comparisons using the Bonferroni correction were performed for multiple comparisons. In addition, categorical variables were showed as number with percent and analyzed by the χ^2 test. Wnt2 and Wnt4 were dichotomized into 2 categories with categorical analysis including higher than median and lower than median. The cumulative incidence of the MACE was determined by the Kaplan−Meier method. Multivariable Cox proportional hazard

regression model was used to assess the hazard ratios (HR) of MACEs associated with Wnt2 and Wnt4 status. Variables (clinically meaningful factors) that had shown $p < 0.10$ in univariate analysis were included into multivariate regression analysis. Spearman's rank correlation coefficient was used to assess the correlation between two indicated factors.

All the experimental data were expressed as mean ± standard error. Unpaired Student's *t* test was carried out to compare statistical differences between two groups. Among multiple groups, the comparisons were performed with one-way ANOVA with Tukey's post-hoc test or two-way ANOVA plus Bonferroni's post hoc.

We used Graphpad Prism version 8.0.1 and SPSS 21.0 to perform cartogram and statistical analysis. A *P* value less than 0.05 was considered to be statistically significant.

2.15. Role of the funding source

The funding agencies were independent from the study design, collection, analysis and interpretation of data, manuscript preparation and the decision to submit the paper for publication.

3. Results

3.1. Serum levels of Wnt2 and Wnt4 are increased in AMI patients

To investigate serum Wnt2 and Wnt4 levels in patients with AMI, a total of 109 patients with clinically diagnosed AMI and 56 age and sex-matched non-AMI patients (See method section) were enrolled in this study. The detailed baseline characteristics of AMI and non-AMI groups are shown in Table 1. AMI patients had higher total triglyceride, LDL-C, HbA1c, uric acid, BNP, cTnI, hs-CRP, and HDL-C concentrations than in non-AMI group (Table 1). Other parameters including SBP or DBP did not show any difference between the two groups. The serum levels of Wnt2 and Wnt4 were higher in the AMI group than in non-AMI group (Wnt2: 1.20 ± 1.28 *vs* 0.818 ± 1.01 ng/mL, $p = 0.046$; Wnt4: 91.2 ± 37.4 *vs* 68.5 ± 40.1 pg/ml, $p < 0.001$, Student's *t* test, Fig. 1a, b).

These data suggested that serum Wnt2 and Wnt4 levels are increased in patients with AMI.

3.2. Elevated serum Wnt2 and Wnt4 are associated with MACEs risk in AMI patients during one-year follow-up

To estimate the prognostic value of elevated serum Wnt2 and Wnt4 levels in AMI patients, we used Kaplan-Meier survival analysis to compare clinical outcomes in AMI patients. Wnt2 and Wnt4 were dichotomized into two categories with categorical analysis including lower than median (low group) and higher than median (high group). In one year of follow-up for 109 AMI patients, there were 16 patients experienced major adverse cardiovascular events (MACEs) from 6 readmissions for unstable angina, 3 readmissions for heart failure, 2 myocardial infarction, 4 stroke and 1 death. Patients with high Wnt2 or Wnt4 level (Wnt2 ≥ 0.86 ng/mL or Wnt4 ≥ 86.2 pg/mL) had more MACEs than those with low expression (Wnt2 < 0.86 ng/mL or Wnt4< 86.2 pg/mL)($p = 0.008$ and 0.03, respectively, the log-rank test, Fig. 1c, d; HR 4.658, 95% CI [1.327, 16.35], $p = 0.016$; or HR 3.161, 95% CI [1.019, 9.803], $p = 0.046$, univariate Cox regression analysis, Table 2). Patients with both high Wnt2 and Wnt4 (Wnt2 ≥ 0.86 ng/mL and Wnt4 ≥ 86.2 pg/mL) had the most significant and increased risk of MACEs (HR 11.17, 95% CI [1.430, 87.31], $p = 0.021$, univariate Cox regression analysis, Table 2). Importantly, after adjustment for age and sex, patients with high Wnt2 (≥ 0.86 ng/mL) or both high Wnt2 and Wnt4 (Wnt2 ≥ 0.86 ng/mL and Wnt4 ≥ 86.2 pg/mL) remained independently related to MACEs risk (HR 4.173, 95% CI [1.178, 14.78], $p = 0.027$;or HR 11.28, 95%CI [1.442, 88.16], $p = 0.021$, multivariable adjusted Cox regression analysis, Table 2). However,

Table 1
Baseline characteristics of AMI patients and non-AMI group.

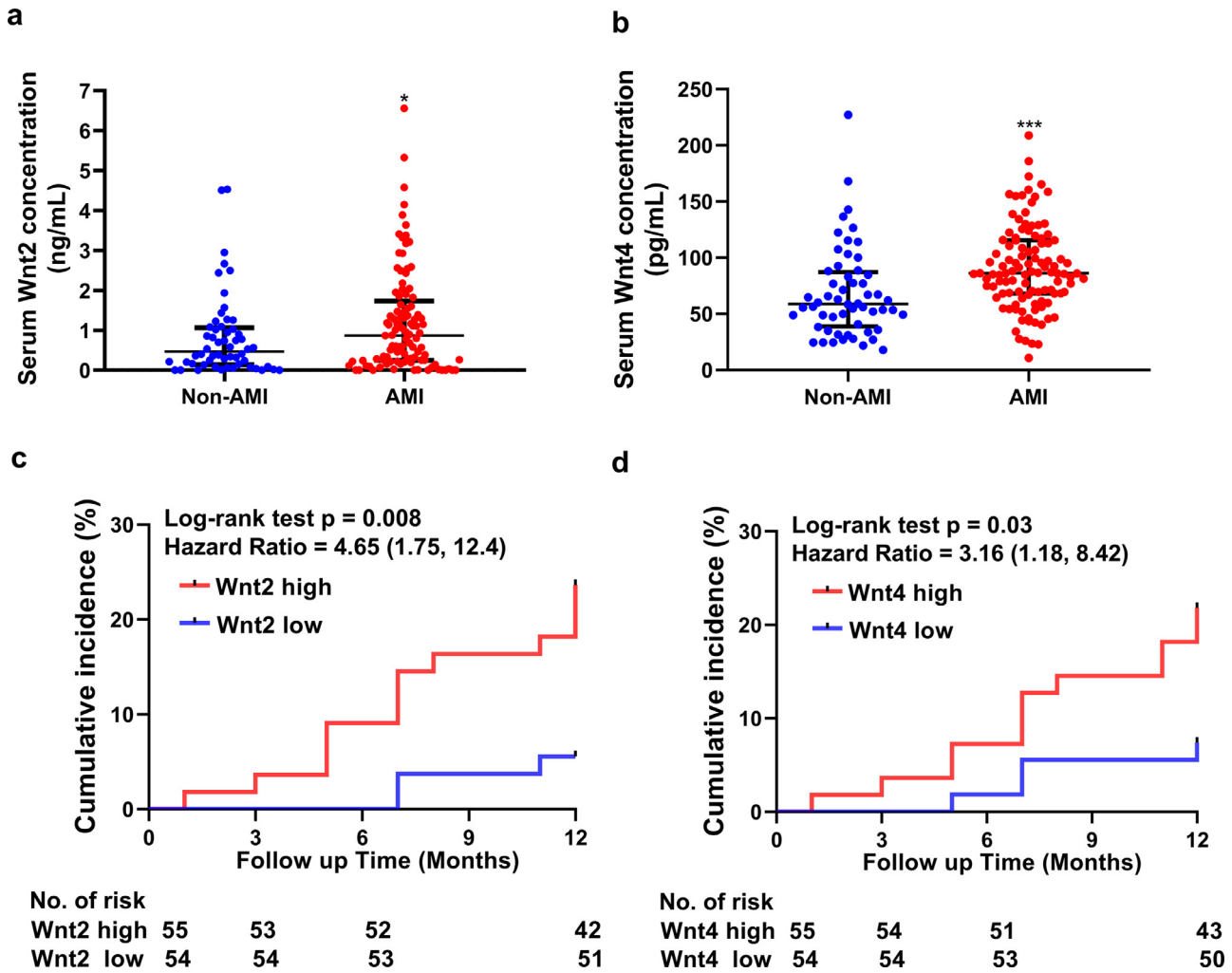|	Non-AMI (*n* = 56)	AMI (*n* = 109)	*p*
Male, *n* (%)	28 (50.0%)	72 (66.1%)	0.064
Age, years, mean ± SD	65.4 ± 9.39	66.1 ± 11.2	0.704
SBP (mmHg), mean ± SD	134.5 ± 16.69	131.0 ± 25.06	0.349
DBP (mmHg), mean ± SD	77.57 ± 10.40	76.82 ± 13.34	0.712
Smoked, *n* (%)	28 (50.0%)	70 (64.2%)	0.095
Medical history			
Diabetes, *n* (%)	23 (41.1%)	43 (39.4%)	0.868
Hypertension, *n* (%)	35 (62.5%)	70 (62.4%)	0.865
Atrial fibrillation, *n* (%)	5(8.93%)	17 (15.6%)	0.334
Chronic Heart failure, *n* (%)	8(14.3%)	27 (24.8%)	0.159
Blood biochemical analysis			
Creatinine (μmol/L) , mean ± SD	72.7 ± 25.8	78.0 ± 19.8	0.304
ALT(U/L), mean ± SD	20.7 ± 12.6	25.3 ± 42.5	0.435
AST(U/L), mean ± SD	19.7 ± 8.25	22.2 ± 12.6	0.113
TC (mmol/L), mean ± SD	4.34 ± 1.23	4.57 ± 1.37	0.174
TG (mmol/L), mean ± SD	1.55 ± 0.939	2.63 ± 1.96	0.001
LDL-C (mmol/L), mean ± SD	2.66 ± 1.02	3.91 ± 2.05	0.001
HDL-C (mmol/L), mean ± SD	1.17 ± 0.31	1.62 ± 1.12	0.004
HbA1c (%), mean ± SD	6.35 ± 1.02	7.04 ± 1.78	0.016
Uric acid (μmol/L) , mean ± SD	306 ± 90.7	366 ± 102	0.001
cTnI (ng/mL), median [inter-quartile range]	0.006[0.004, 0.007]	0.394[0.012, 9.17]	0.001
BNP (pg/L), median [inter-quartile range]	70.5[45.9, 97.9]	100.5[57.1, 210.5]	0.003
hs-CRP (mg/L), median [interquartile range]	0.728[0.303, 2.21]	3.86 [1.01, 7.36]	0.001
Medication on admission			
Aspirin, *n* (%) β-blocker, *n* (%)	7(12.5%)	9 (8.25%)	0.412
ACEIs or ARBs, *n* (%)	12(21.4%)	28 (25.7%)	0.572
Aspirin, *n* (%)	21(37.5%)	38 (34.9%)	0.867
Statin, *n* (%)	21(37.5%)	36 (33.0%)	0.606
Echocardiographic parameters			
LAD (mm), mean ± SD	36.1 ± 4.52	36.9 ± 4.54	0.283
LVEF (%), mean ± SD	57.2 ± 2.78	53.9 ± 7.54	0.004
LVED (mm), mean ± SD	44.0 ± 4.43	47.4 ± 5.02	0.001
IVS (mm), mean ± SD	10.5 ± 1.01	11.1 ± 1.15	0.004
LVPW (mm), mean ± SD	10.4 ± 0.906	10.9 ± 1.12	0.011

Data are expressed as Mean ± SD, *n* (%) or median [interquartile range]. TC, total cholesterol; TG, total triglyceride; HDL, high-density lipoprotein; LDL, low-density lipoprotein; AST, aspartate aminotransferase; ALT, alanine aminotransferase; hs-CRP, high-sensitivity C-reactive protein; ARB, angiotensin receptor blockers; ACEI, angiotensin converting enzyme inhibitor; LVED, Left ventricular end diastolic diameter; LVEF, Left ventricular ejection fraction; LAD, Left atrium diameter; LVPW, left ventricular posterior wall; IVS, interventricular septum. Statistics: Student's *t* test was used for normally distributed variables; Mann-Whitney U test was used for skewed variables, and χ^2 test was used for categorical variables.

serum Wnt2 or Wnt4 level was not correlated with age, smoker, blood pressure and echocardiographic parameters including left ventricular ejection fraction (LVEF); left ventricular end diastolic diameter (LVED) and inter-ventricular septum (IVS) (Table S3).

Thus, elevated Wn2 and Wnt4 levels may increase the risk for worse outcome in AMI patients.

3.3. Serum and cardiac Wnt2 and Wnt4 are increased at early-phase following experimental MI

We then examined cardiac and serum Wnt2 and Wnt4 levels at different time-points (3d, 7d, 14d and 28d) in mice post-MI. Col1, Col3 (fibrotic-related proteins) and transforming growth factor-β1 (TGF-β1, pro-fibrotic protein) were increased from 3 days and peaked at 7 days in the border zone post-MI compared with sham group (Fig. 2a). Cardiac Wnt2 and Wnt4 were significantly increased at 3 days and decreased at 7 days, then recovered from 14 days to 28 days in the border zone of infarct area, while were greatly decreased from 7 days in infarct area, compared with sham group

a

b

c

Log-rank test p = 0.008
Hazard Ratio = 4.65 (1.75, 12.4)

Wnt2 high
Wnt2 low

No. of risk

Wnt2 high	55	53	52	42
Wnt2 low	54	54	53	51

d

Log-rank test p = 0.03
Hazard Ratio = 3.16 (1.18, 8.42)

Wnt4 high
Wnt4 low

No. of risk

Wnt4 high	55	54	51	43
Wnt4 low	54	54	53	50

Fig. 1. Serum Wnt2 and Wnt4 are increased in patients with AMI and correlated to the increased risk of adverse outcomes of patients (a, b) ELISA analysis of serum Wnt2 and Wnt4 level in a total of 109 patients with AMI and 56 non-AMI patients. Data are expressed as means±SD, $*p < 0.05$, $** p < 0.01$, $*** p < 0.001$ by Student's t test. (c, d) Kaplan−Meier incidence of MACEs in one year according to high or low level of serum Wnt2 or Wnt4. Wnt2 and Wnt4 were dichotomized into 2 categories with categorical analysis including higher than median and lower than median. Wnt2 high: ≥0.86 (ng/mL); Wnt2 low: < 0.86(ng/mL); Wnt4 high:≥86.2(pg/mL); Wnt4 low: < 86.2(pg/mL). MACEs: major adverse cardiovascular events. Estimated HR, 95% CIs, and p values were calculated. Statistics: The cumulative incidence of the MACE was determined by the Kaplan−Meier method, and the difference between groups was compared using the log-rank test. MACEs: major adverse cardiovascular events. Estimated HR, 95% CIs, and p values were calculated.

Table 2
Univariate and multivariable adjusted Cox proportional hazard regression models of incident MACEs with serum Wnt2 and Wnt4 in AMI patients.

	No. of Patients	No. of MACEs	Model 1 HR (95% CI)	Model 2 HR (95% CI)
Wnt2(ng/mL)				
< 0.86	54	3	1	1
≥0.86	55	13	4.658 [1.327, 16.35]*	4.173 [1.178, 14.78]*
Wnt4(pg/mL)				
< 86.2	54	4	1	1
≥86.2	55	12	3.161 [1.019, 9.803]*	2.569 [0.812, 8.126]
Wnt2(ng/mL) and Wnt4(pg/mL)				
< 0.86 and <86.2	31	1	1	1
≥0.86 and <86.2	23	3	4.194[0.436,40.33]	4.508[0.462,44.02]
<0.86 and ≥86.2	23	2	2.733[0.248,30.14]	2.800[0.253,30.94]
≥0.86 and ≥86.2	32	10	11.17[1.430, 87.31]*	11.28[1.442, 88.16]*

Model1: Univariate model. Model2: Multivariable model. *P<0.05. Statistics: Multivariable adjusted Cox regression analysis.

(Figs. 2a. S1a). Serum Wnt2 and Wnt4 were sharply increased from 3 days and maintained high level until 28 days post-MI, compared with sham group (Fig. 2b). It suggested that two proteins may be involved in cardiac remodeling outside the infarct area post-MI.

We also detected the expression and secretion of Wnt2 and Wnt4 in neonatal rat cardiomyocytes (NRCMs) and cardiac fibroblasts (NRCFs), under hypoxia, respectively. Wnt2 and Wnt4 were greatly increased in NRCFs from 6 h, while increased in NRCMs from 3 h,
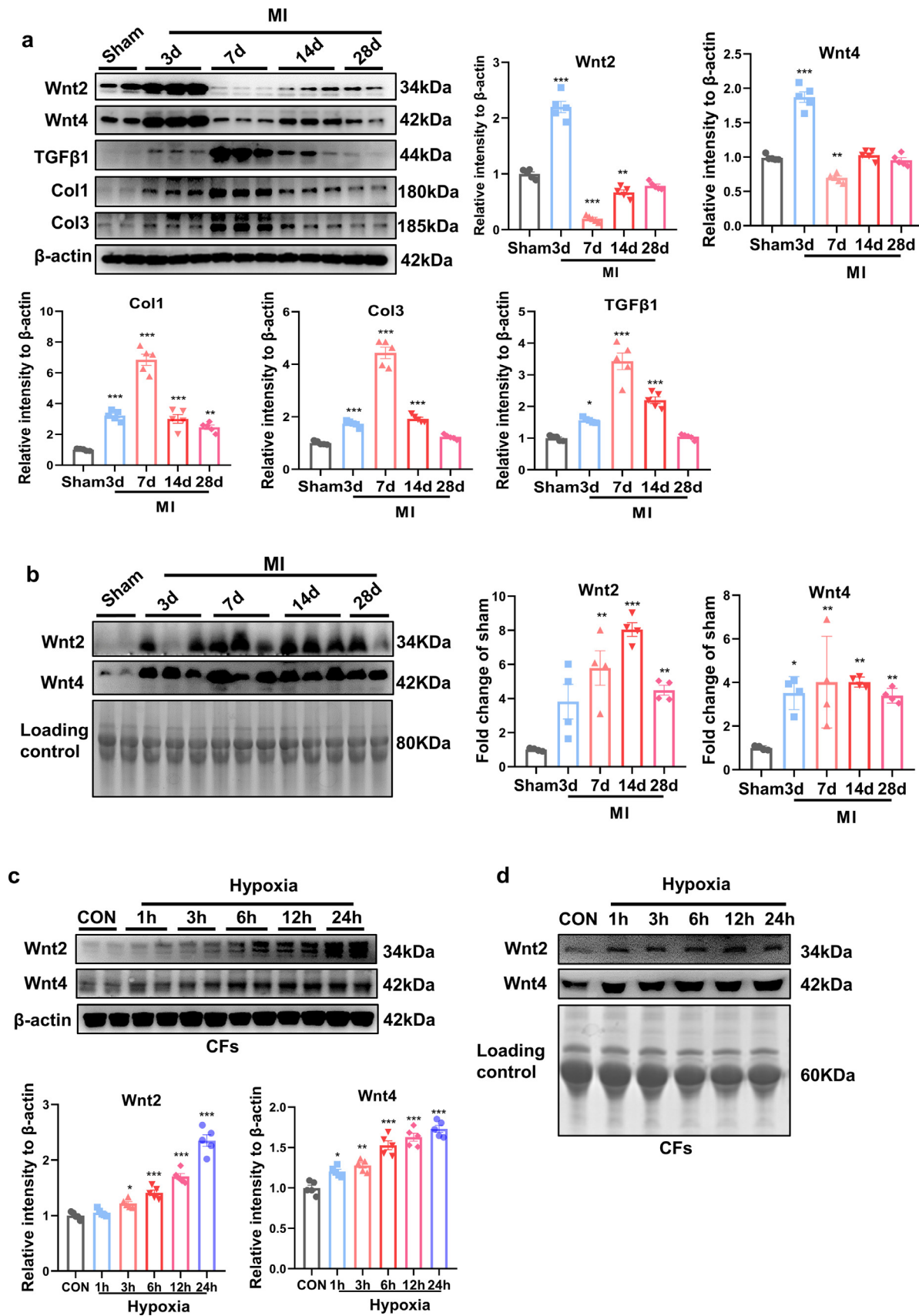
Fig. 2. Serum and cardiac Wnt2 and Wnt4 levels are increased in mice following MI. (a) Western blot analysis of the expression of Wnt2, Wnt4, Col1, Col3 and TGF-β1 in the border zone of infarcted area at different time-points (3d, 7d, 14d, 28d) following MI. Sham operation was used as control. Values were expressed as means±S.E.M; * $p < 0.05$, ** $p < 0.01$, *** $p < 0.001$ vs sham group, $n = 5$/group. (b) Western blot analysis of serum Wnt2 and Wnt4 from sham group and different time-points (3d,7d,14d,28d) after MI. Values were expressed as means±S.E.M; * $p < 0.05$, ** $p < 0.01$, *** $p < 0.001$ vs sham group, $n = 4$/group. (c) Wnt2 and Wnt4 expression were analyzed by Western blot analysis in cultured neonatal rat cardiac fibroblasts (NRCFs) at different time-points (1 h,3 h,6 h,12 h,24 h) in response to hypoxia. Normaxia group was used as control. Values were expressed as means±S.

after hypoxia, compared with their control group, respectively (Figs. 2c, S2a). In conditional medium from NRCMs or NRCFs, Wnt2 and Wnt4 levels were increased from 1 h and maintained at high level until 24 h after hypoxia (Figs. 2d, S2b).

Wnt5a [25] or Wnt11 [11] is elevated in myocardium from heart failure patients or experimental MI. Serum Wnt11 level did not alter in AMI patients compared with control group in our preliminary experiment (Fig. S1b). In the border zone of infarcted area following MI, Wnt5a decreased in time-dependent manner, but Wnt11 showed no obvious change following MI (Fig S1c). These data indicated that Wnt5a or Wnt11 may have few effects in cardiac remodeling following MI.

These data suggested elevated Wnt2 and Wnt4 from cardiac myocytes or fibroblasts may be critical for cardiac remodeling after MI.

3.4. Knockdown of Wnt2 and Wnt4 improve cardiac function and attenuate cardiac remodeling following MI

To explore the role of the increased Wnt2 and Wnt4 post-MI, we knocked-down Wnt2 and Wnt4 by injection of shWnt2/4-AAV9 by tail vein in mice at 3 weeks before MI. shScramble-AAV9 (shNC) was injected as control. Cardiac function was analyzed by echocardiography analysis at 0 day (before MI operation), 7 days, 14 days and 28 days after MI. Acute isolated cardiomyocytes and cardiac fibroblasts from shWnt2/4-injected mice showed the lower expression of Wnt2 or Wnt4 than those in shNC-injected mice after sham operation or MI (Fig S3a). ShWnt2/4-AAV9 injection induced the decreased cardiac but not liver expression of Wnt2 and Wnt4 after sham or MI operation (Figs. 3a, S3b). MI mediated the decreased EF or FS, the increased the left ventricle systolic or diastolic dimension (LVIDs or LVIDd), end-diastolic volume (EDV) and end-systolic volume (ESV) at different-time points, but the effects were significantly improved by shWnt2/4-AAV9 injection (Figs. 3b, S4a). There is no difference in heart rate between the two groups (Fig. S4a). Hemodynamic analysis revealed that shWnt2/4 greatly inhibited the decreased dp/dt or the increased LVEDP, -dp/dt and Tau following MI (Fig 3c). ShWnt2/4 also attenuated the increased lung weight/body weight (LW/BW), indicating improvement of pulmonary edema (Fig. S4b). Further analysis indicated that shWnt2/4-AAV9 injection significantly reduced the fibrosis area, inhibited the increased expression of Col1, Col3, α-SMA, MMP2 and MMP9 at 28 days after MI (Fig. 3d, e). In addition, shWnt2/4 attenuated the increased heart weight/ body weight (HW/ BW), cross section area (CSA) of cardiomyocytes and the mRNA levels of NPPA and NPPB (hypertrophic genes) after MI (Fig. S4b–d), suggesting shWnt2/4 improves cardiac hypertrophy following MI.

These data suggested that elevated Wnt2 and Wnt4 are critical for cardiac remodeling and dysfunction following MI

3.5. Wnt2 or Wnt4 induces pro-fibrotic effects in response to hypoxia

Wnt-C59, a Wnt-secretion inhibitor, greatly inhibited the increased expression of Col1, Col3, α-SMA,TGFβ1, MMP9, MMP2 and active β-catenin induced by hypoxic stimulation in NRCFs (Fig. S5), suggesting that Wnt secretion is involved in cardiac fibrosis following MI. To explore the role of Wnt2 or Wnt4 in the pro-fibrotic effects induced by hypoxia, we knocked down the expression of Wnt2 or Wnt4 by transfection of si-Wnt2 or si-Wnt4 into NRCFs to detect fibrotic-related proteins under hypoxia. Si-Wnt2 or si-Wnt4 significantly attenuated the increased expression of Col1, Col3, TGF-β1, MMP2, MMP9, alpha-smooth muscle actin (α-SMA) and p-Smad2/3

induced by hypoxia in NRCFs (Fig. 4a, b). However, si-Wnt2 or si-Wnt4 did not affect the increased expression of connective tissue growth factor (CTGF, a pro-fibrotic mediator) under hypoxia (Fig. 4a, b). The scratch assay revealed hypoxia promoted migration of fibroblasts, but the speed was lower in si-Wnt2 or si-Wnt4 group than in si-Scram group over 12 h (Fig. 4c).

Exogenous human recombinant Wnt2 or Wnt4 were added into NRCFs at different concentrations to observe the pro-fibrotic roles. The expression of Col1, Col3, TGF-β1, MMP2,MMP9, p-Smad2/3 and active β-catenin were enhanced by Wnt2 or Wnt4 in concentration-dependent manner in NRCFs (Fig. S6a). But, Wnt2 or Wnt4 showed few effects on CTGF expression at any concentration (Fig. S6b). In adult mouse cardiac fibroblasts (AMCFs), Wnt2 or Wnt4 showed the similarly pro-fibrotic effects evidenced by the increased expression of Col1, Col3, TGF-β1 and MMP2 in concentration-dependent manner (Fig. S6c). The scratch assay revealed that the migration speed of NRCFs was higher in Wnt2 or Wnt4 group than in PBS group over 12 h (Fig. S6d), suggesting Wnt2 or Wnt4 promotes the migration of cardiac fibroblasts.

But in cultured NRCMs, Wnt2 or Wnt4 did not increase the hypertrophic genes expression at any concentration (Fig. S7), suggesting Wnt2 or Wnt4 may not directly act on cardiomyocytes to promote hypertrophic response.
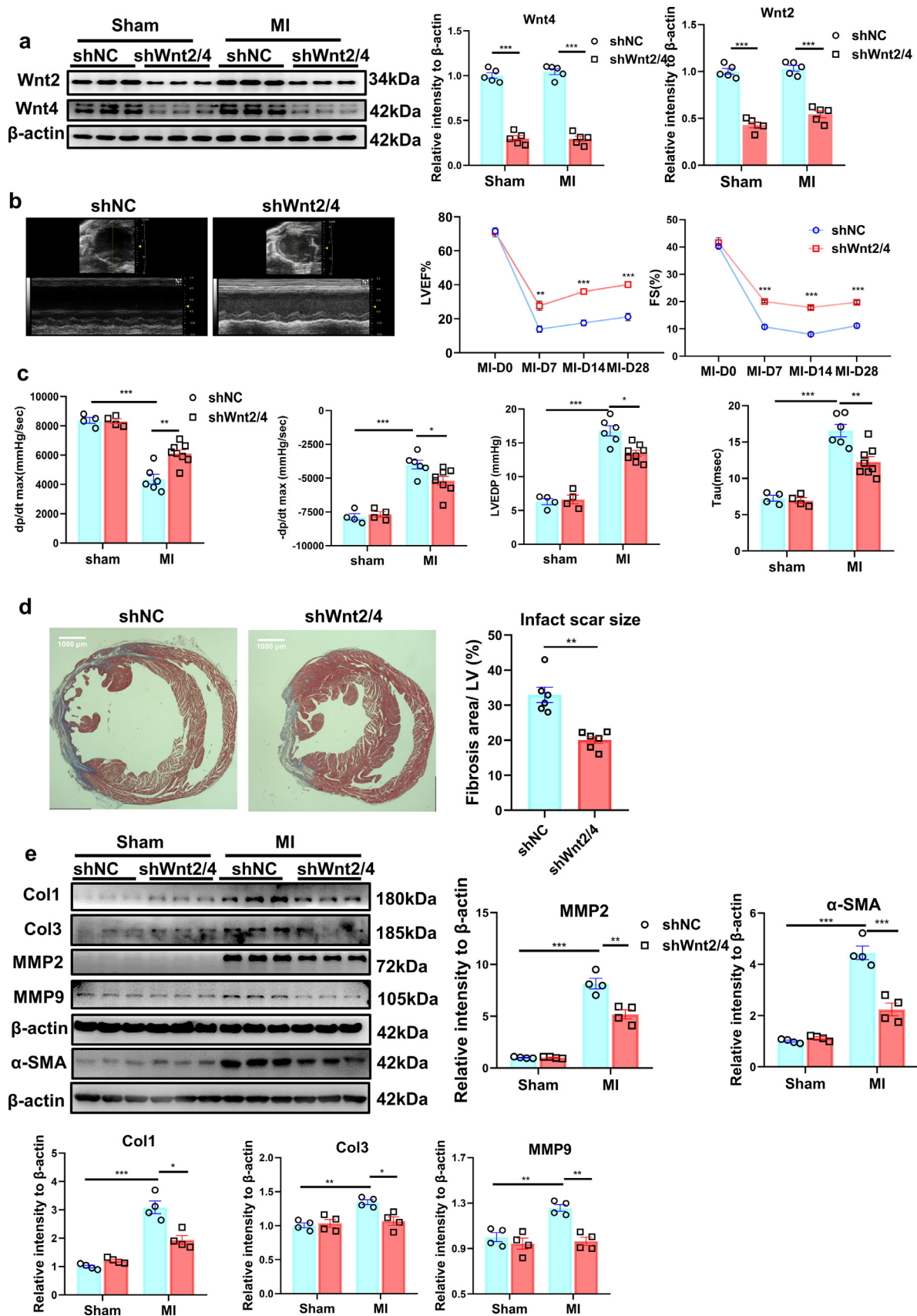
These data indicated that Wnt2 or Wnt4 is involved in the pro-fibrotic effects in cardiac fibroblasts under hypoxia.

3.6. Wnt2 and Wnt4 activate β-catenin and NF-κB signaling, and upregulate Fzd receptor in neonatal rat cardiac fibroblasts

The activation of β-catenin or NF-κB signaling is involved in cardiac fibrosis in response to multiple stimulations [26,27]. Wnt2 and Wnt4 directly promoted the activation of β-catenin in NRCFs (Fig. S6a). TOPflash luciferase reporter assay revealed that the transcriptional activity of T-cell factor (TCF)/lymphoid enhancer factor (LEF) was increased by human recombinant Wnt2 or Wnt4 stimulation (Fig. S8a).The increased p-p65 level, marked the activation of NF-κB, was observed from 3 days post-MI (Fig. S9). Exogenous human recombinant Wnt2 and Wnt4 increased p-p65 level in cultured NRCFs from 15 min and 30 min after treatment, respectively (Fig. S8b). The active β-catenin or the p-p65 enters into nucleus to initiate target genes transcription. We examined β-catenin or p65 level in nucleus and cytoplasm in NRCFs treated with Wnt2 or Wnt4. The expression of β-catenin or p65 level was enhanced in nucleus while decreased in cytoplasm in NRCFs stimulated with Wnt2 or Wnt4 (Fig. S8c,d), indicating Wnt2 or Wnt4 promotes translocation of β-catenin and p65 from cytoplasm to nucleus.

Cycloheximide (for stop protein translation) treatment did not affect the activation of β-catenin and NF-κB mediated by Wnt2 or Wnt4 (Fig. S8e),indicating the primary effects of Wnt2 or Wnt4 in NRCFs. Hypoxia induced the increased expression of p-p65, the effect was greatly suppressed by transfection of si-Wnt2 or si-Wnt4 in NRCFs (Fig. 5a). Similarly, the translocation of β-catenin and p65 from cytoplasm to nucleus induced by hypoxia was inhibited by si-Wnt2 or si-Wnt4 transfection (Figs. 5b, S8f). The results suggested that Wnt2 or Wnt4 promotes cardiac fibrosis by β-catenin and NF-κB signaling.

Wnt-signaling was often induced by Fzd receptors [8]. Fzd2 or Fzd4 was increased in the border zone of infarcted area from 3 days to 7 days post-MI (Fig. S9). In cultured NRCFs, Fzd2 and Fzd4 proteins or mRNAs was increased by Wnt2 or Wnt4 treatment (Fig. S10a, b).

E.M; * $p < 0.05$, ** $p < 0.01$, *** $p < 0.001$ vs control group. n = 4/group. (d) The representative images of Wnt2 and Wnt4 expression with Western blot analysis in conditional medium from neonatal rat cardiac fibroblasts (NRCFs) of control group and at different time-points (1 h,3 h,6 h,12 h,24 h) after hypoxia. In (b) and (d), a conventional Coomassie staining of polyvinylidene fluoride (PVDF) membranes showed the total protein load which was as the internal control (Loading control). The experiment was repeated for three times. MI: Myocardial infarction; CON: control. Statistics: One-way ANOVA with post-hoc Tukey test.

Fig. 3. Knockdown of Wnt2/Wnt4 suppresses cardiac dysfunction and fibrosis post-MI. 8-10 weeks old male mice were injected with shWnt2/4-AAV9 (shWnt2/4) or shScramble-AAV9 (shNC, as control) by tail vein at 3 weeks before sham or MI operation. (a) Wnt2 and Wnt4 levels were determined in the non-infarcted area by western blot method on day 28 post-MI. Values were expressed as means±S.E.M; *** $p < 0.001$ vs shNC group; n = 5/each group. Statistics: Two-way ANOVA with a Bonferroni post hoc test. (b) Echocardiographic analysis of mice at day 0, day7, day14 and day28 after MI. Left lane: Representative images of M-mode echocardiogram captured on the 28th day post-MI. Right lane: quantitative analysis of LVEF, FS; LVEF: Left ventricular ejection fraction; FS, fraction shortening. Values were presented as means±S.E.M. * $p < 0.05$, ** $p < 0.01$, *** $p < 0.001$ vs shNC

Hypoxia induced the increased expression of Fzd2 and Fzd4, which were greatly suppressed by transfection of si-Wnt2 or si-Wnt4 into NRCFs (Fig. 5a). *In vivo*, AAV9-mediated knockdown of Wnt2/4 inhibited the increased expression of p-p65, but did not affect Fzd2 and Fzd4 level in the border zone of infarcted area following MI (Fig. 5c).

These data suggested that NF-κB activation or Fzd4/2-mediated signaling may be involved in the cardiac fibrosis induced by Wnt2 and Wnt4 following MI.

3.7. NF-κB inhibitor attenuates the pro-fibrotic effects induced by Wnt2 or Wnt4

NF-κB inhibitor, JSH23 or neferine (5μM), was added into NRCFs treated with human recombinant Wnt2 or Wnt4. JSH23 or Neferine greatly inhibited the increased p-p65 level mediated by Wnt2 or Wnt4 (Figs. 6a, b; S11). As expected, Wnt2 or Wnt4 induced the increased expression of Col1, Col3, p-p65, MMP2 and MMP9, which were partly abolished by JSH23 or neferine in cultured NRCFs (Figs. 6a, b; S11). However, the inhibitor did not affect the increased expression of active β-catenin induced by Wnt2 or Wnt4 in NRCFs (Figs. 6a, b; S11).

The data indicated that Wnt2 or Wnt4 mediated cardiac fibrosis by activation of NF-κB signaling.

3.8. Inhibition of Wnt/β-catenin signaling attenuates the activation of NF-κB and pro-fibrotic effects induced by Wnt2 or Wnt4

We treated ICG-001, a specific inhibitor of canonical Wnt/β-catenin signaling, into NRCFs, to detect the activation of NF-κB and pro-fibrotic effects induced by human recombinant Wnt2 or Wnt4. ICG-001 greatly inhibited the increased active β-catenin and p-p65 level caused by Wnt2 or Wnt4 (Fig 7a,b). Wnt2 or Wnt4 induced pro-fibrotic effects evidenced by the enhanced Col1, Col3, TGF-β1 expression, these effects were significantly attenuated by ICG-001 treatment (Fig 7a,b). However, ICG-001 did not affect the expression of Fzd2 or Fzd4 in Wnt2- or Wnt4-treated-NRCFs (Fig 7a,b).

These data suggested Wnt2 or Wnt4 induces pro-fibrotic effects by activation β-catenin/NF-κB signaling.

3.9. Si-Fzd2 or si-Fzd4 inhibits the activation of NF-κB and pro-fibrotic effects induced by Wnt4 or Wnt2 respectively

To explore whether Fzd2 or Fzd4 mediates Wnt2 or Wnt4 signaling in cardiac fibrosis, we transfected si-Fzd2 or Fzd4 into NRCFs. Si-Fzd2 or Fzd4 significantly down-regulate the expression of Fzd2 or Fzd4, respectively (Figs. 8a,b; S12,S13). Si-Fzd2 greatly suppressed the activation of NF-κB/p-65, and the increased expression of Col1, Col3, TGF-β1, MMP9 and MMP2, induced by Wnt4 (Fig. 8a), but did not affect the pro-fibrotic effects induced by Wnt2 (Fig. S12).

Si-Fzd4 attenuated the pro-fibrotic effects induced by Wnt2 but not Wnt4 (Figs. 8b; S13). In addition, si-Fzd2 or si-Fzd4 showed few effects on the activation of β-catenin mediated by Wnt2 or Wnt4 (Figs. 8a,b, S13).

These data revealed that Wnt2 and Wnt4 activated NF-κB to promote cardiac fibrosis by Fzd4 and Fzd2 receptor signaling, respectively.

3.10. ShLRP6 inhibits the activation of β-catenin and NF-κB, and pro-fibrotic effects induced by Wnt2 or Wnt4

Wnt2 or Wnt4 increased the expression of LRP6, an essential co-receptor of the Wnt/β-catenin pathway [28], in NRCFs (Fig 9a, b). ShLRP6-lentivirus transfection effectively decreased LRP6 expression in NRCFs, attenuated the activation of β-catenin and NF-κB/P65 induced by Wnt2 or Wnt4. Similarly, shLRP6 inhibited the increased expression of Col1, Col3 and TGF-β1 caused by Wnt2 or Wn4 (Fig 9a, b).

These data indicated that Wnt2 or Wnt4 activates β-catenin/NF-κB to enhance cardiac fibrosis dependently on LRP6 receptor signaling.

4. Discussion

In the study, our novel findings include: (1) Elevated serum Wnt2 and Wnt4 levels positively correlated to adverse outcome in AMI patients. (2) Wnt2 and Wnt4 are early molecules with critical function to initiate cardiac fibrosis following MI. (3) Wnt2 and Wnt4 promote fibrotic effects by activation β-catenin/NF-κB signaling by co-operation of Fzds and LRP6 in cardiac fibroblasts following experimental infarction (Fig. 10). These results suggested that blockade of Wnt2 or Wnt4 signaling may contribute to treatment of cardiac fibrosis following MI.

MI causes cardiomyocyte necrosis, inflammation and fibrosis, leading to the formation of a scar. Following MI, the initial reparative fibrosis prevents rupture of the ventricular wall. But ischemic stress also induces biomechanical or biochemical changes in injured ventricular tissues eliciting a reactive remodeling including interstitial fibrosis [29]. Increasing evidences reveal that Wnt signaling activated following MI [11]. It has been evidenced patients with severe cardiac fibrosis had the highest MACE, even in the absence of coronary artery disease (CAD) [30]. In the present study, AMI patients had significantly higher levels of serum Wnt2 and Wnt4 levels than controls. Elevated serum Wnt2 and Wnt4 are prognostic for one year MACEs (even after adjustment for age and sex). Our data have emphasized the importance of increased serum Wnt2 and Wnt4 concentration in predicting the risk of future cardiovascular events post-MI, indicating a direct association between the pathophysiological roles of Wnt2 or Wnt4 and MI-induced cardiac injury.

Tumor associated fibroblasts secreted-Wnt2 accelerates tumor progression and invasion in multiple cancers [31]. Wnt4 enhances inflammatory response in chronic obstructive pulmonary disease [32]. Wnt2 or Wnt4 promotes smooth muscle cell proliferation and migration, leading to intimal thickening [33,34]. Cardiac Wnt2 or Wnt4 expression was at peak at day3 after MI, whereas in the serum the peak was observed at 14 days post-MI (Wnt2) and 7−14 days post-MI (Wnt4), respectively. *In vitro*, we found hypoxia induced the increased expression and secretion of Wnt2 or Wnt4 from cardiomyocytes and fibroblasts. After a palmitoleate modification, cellular Wnt proteins were released into extracellular space on membrane-bound structures [35]. Wnt ligands traveling on exosomes are involved in the maladaptive cardiac remodeling [36]. It is possible that Wnt2 or Wnt4 is released into circulation in the similar manner post-MI. Considering about 4 h-hall-life of Wnt1 [37], Wnt2 or Wnt4 may have short half-life. The elevated circulation Wnt2 and Wnt4 level may come from the continuously secretion of cardiac cells after MI. Knockdown of Wnt2 and Wnt4 significantly improved cardiac
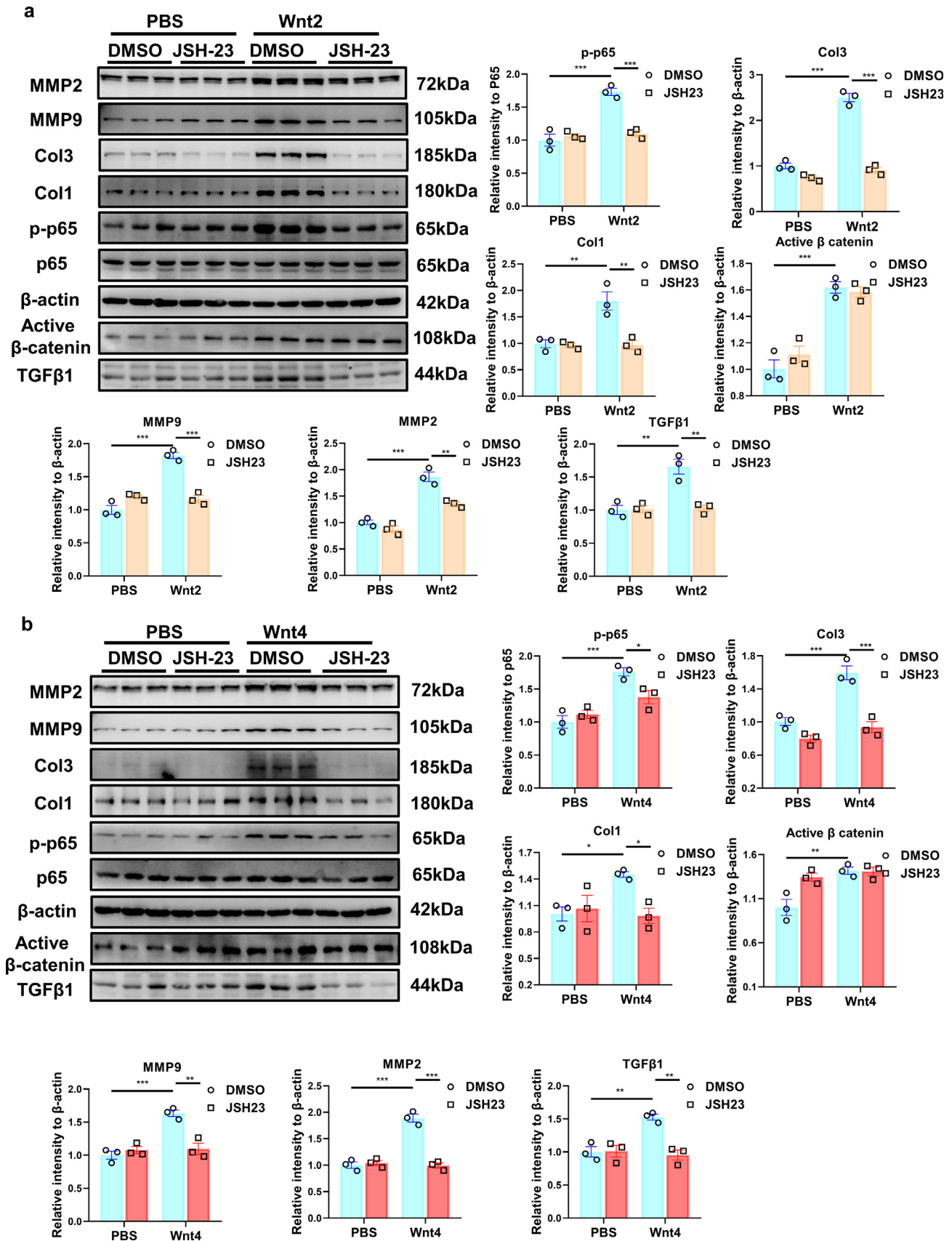
group; *n* = 6/group. Statistics: Student's *t* test. (c) Hemodynamics analysis of dp/dt, -dp/dt, LVEDP and Tau at 21 days after MI in mice. Values were expressed as means±S.E.M. * *p* < 0.05;** *p* < 0.01;*** *p* < 0.001, *n* = 4-8 in each group. Statistics: Two-way ANOVA with a Bonferroni post hoc test. (d) Cardiac fibrosis was examined by Masson staining at 28 days after MI in mice. Bar =1000 μm. Values were expressed as means±S.E.M. ** *p* < 0.01 vs shNC group, *n* = 6 in each group. Statistics: Student's *t* test. (e) Col1, Col3, MMP2, MMP9 and α-SMA protein levels were analyzed by Western blot in border zone of infarcted area on day 28 post-MI. Values were presented as means±S.E.M .* *p* < 0.05, ** *p* < 0.01, *** *p* < 0.001; *n* = 4 in each group. Statistics: Two-way ANOVA with a Bonferroni post hoc test.
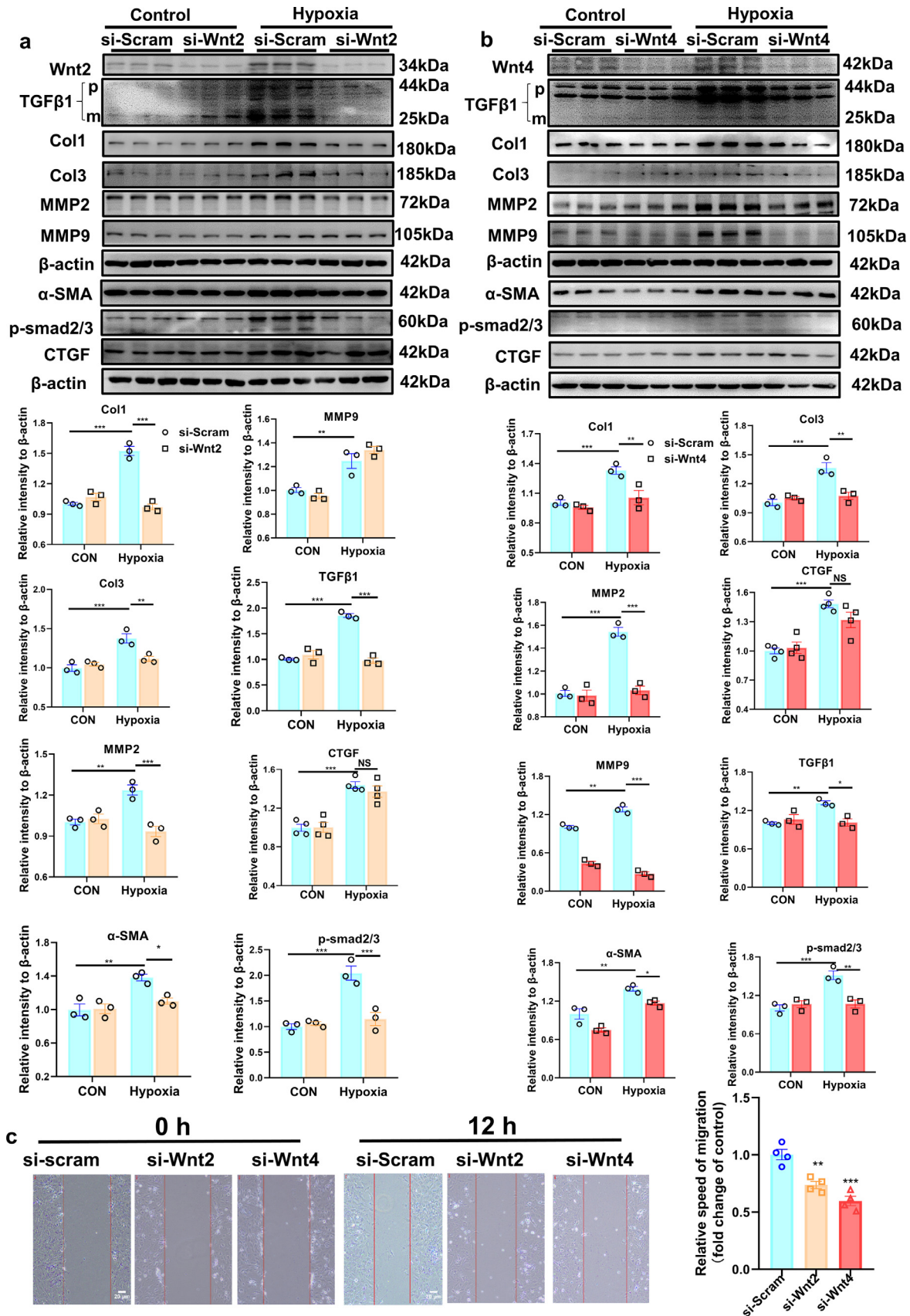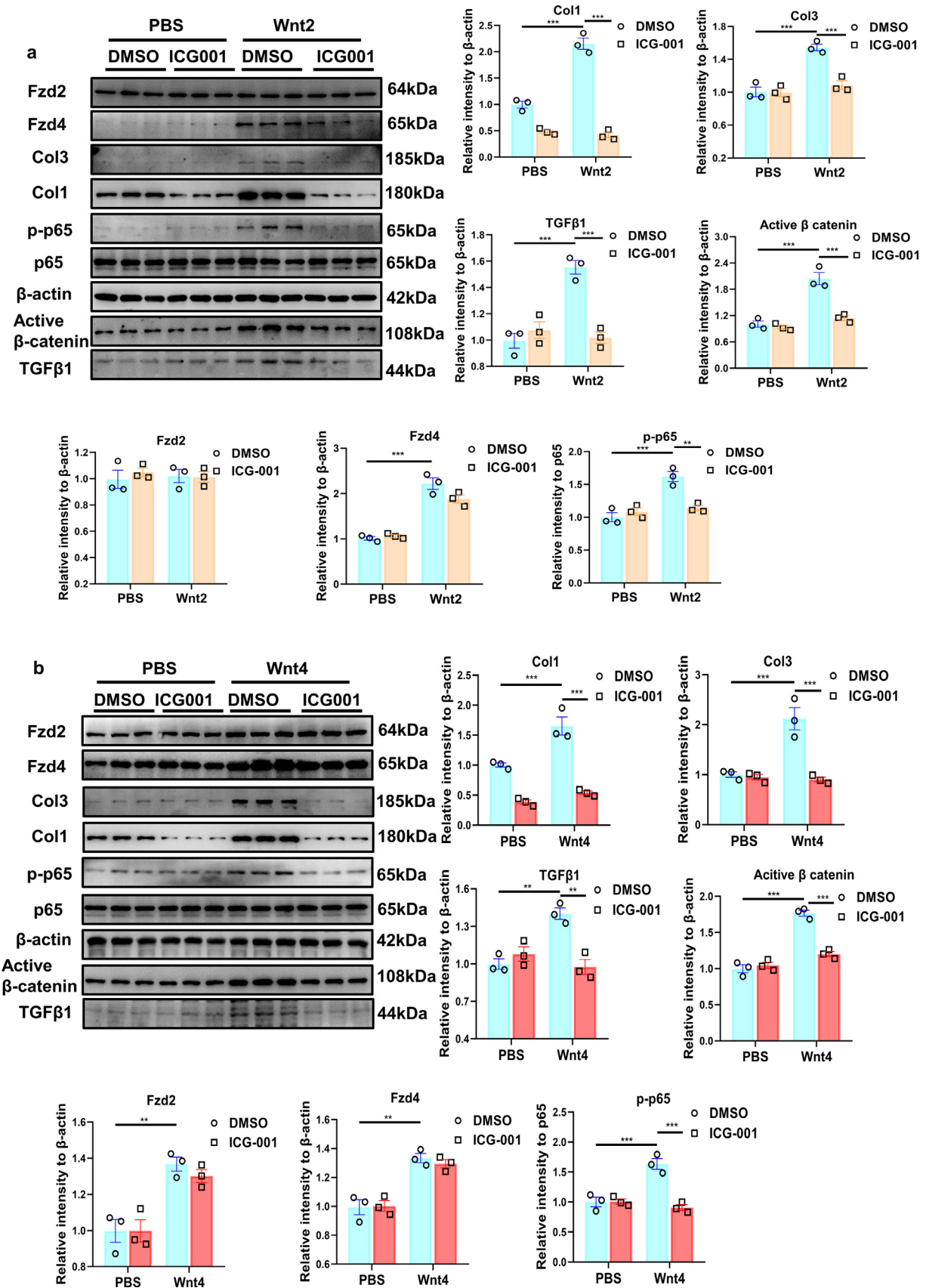
Fig. 4. Wnt2 or Wnt4 is involved in fibroblasts activation in response to hypoxia. (a,b) Western blot analysis of the expressions of Wnt2, Wnt4, Col1, Col3, TGFβ1, MMP9 MMP2, p-smad2/3, CTGF and α-SMA protein in neonatal rat cardiac fibroblasts (NRCFs). These NRCFs were pretreated with siRNA targeted Wnt2 or Wnt4 (si-Wnt2 or si-Wnt4) or si-Scramble (si-Scram) for 24 h, and then exposed to hypoxia or normoxia (Control) for 3 h. p: pro-TGF-β1; m: mature or active TGF-β1; TGF-β1 mature form was analyzed. Values were described as means±S.E.M; * $p < 0.05$, ** $p < 0.01$, *** $p < 0.001$; n = 3/group. Statistics: Two-way ANOVA with a Bonferroni post hoc test. c: Scratch assay for migratory ability of cardiac fibroblasts
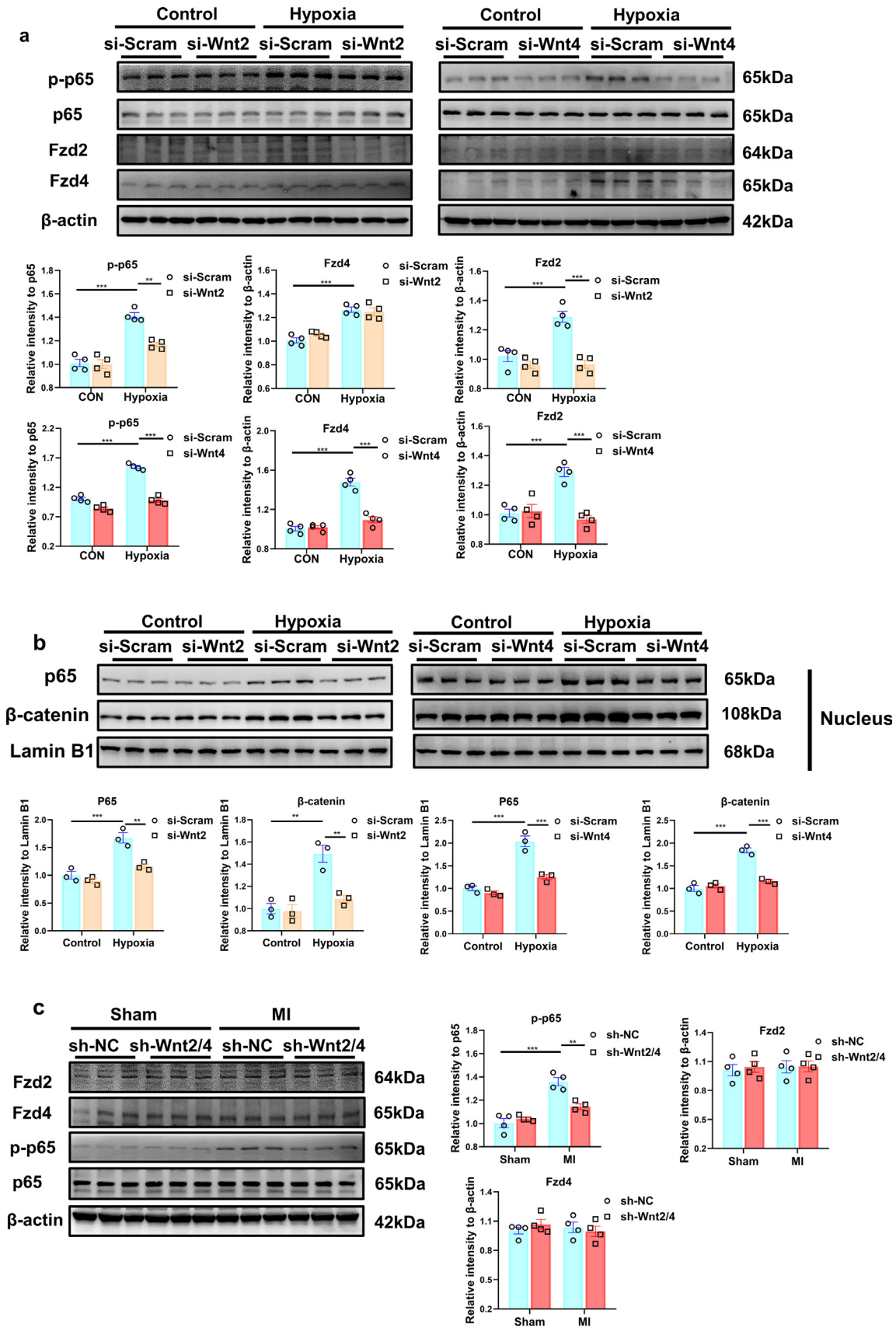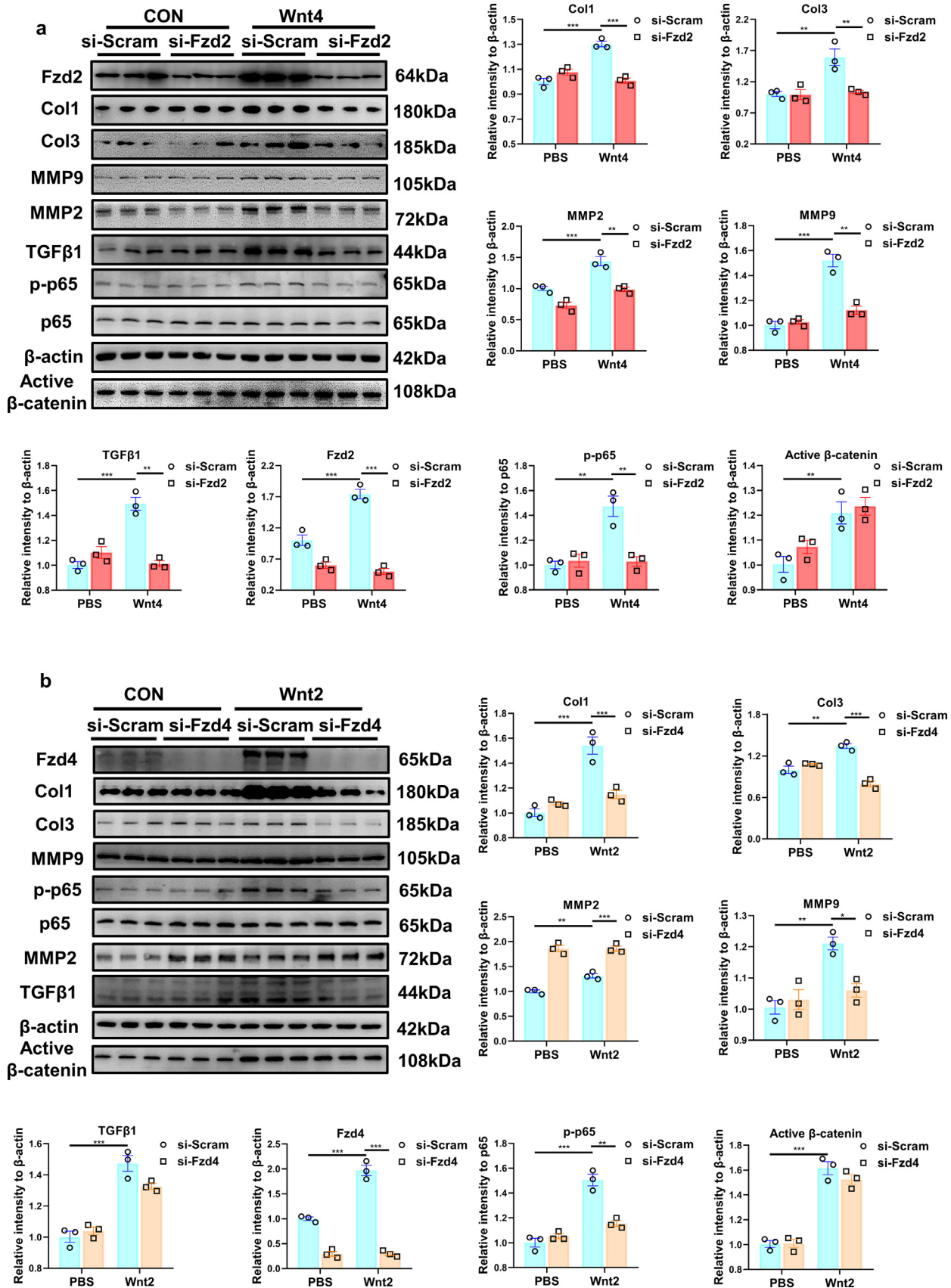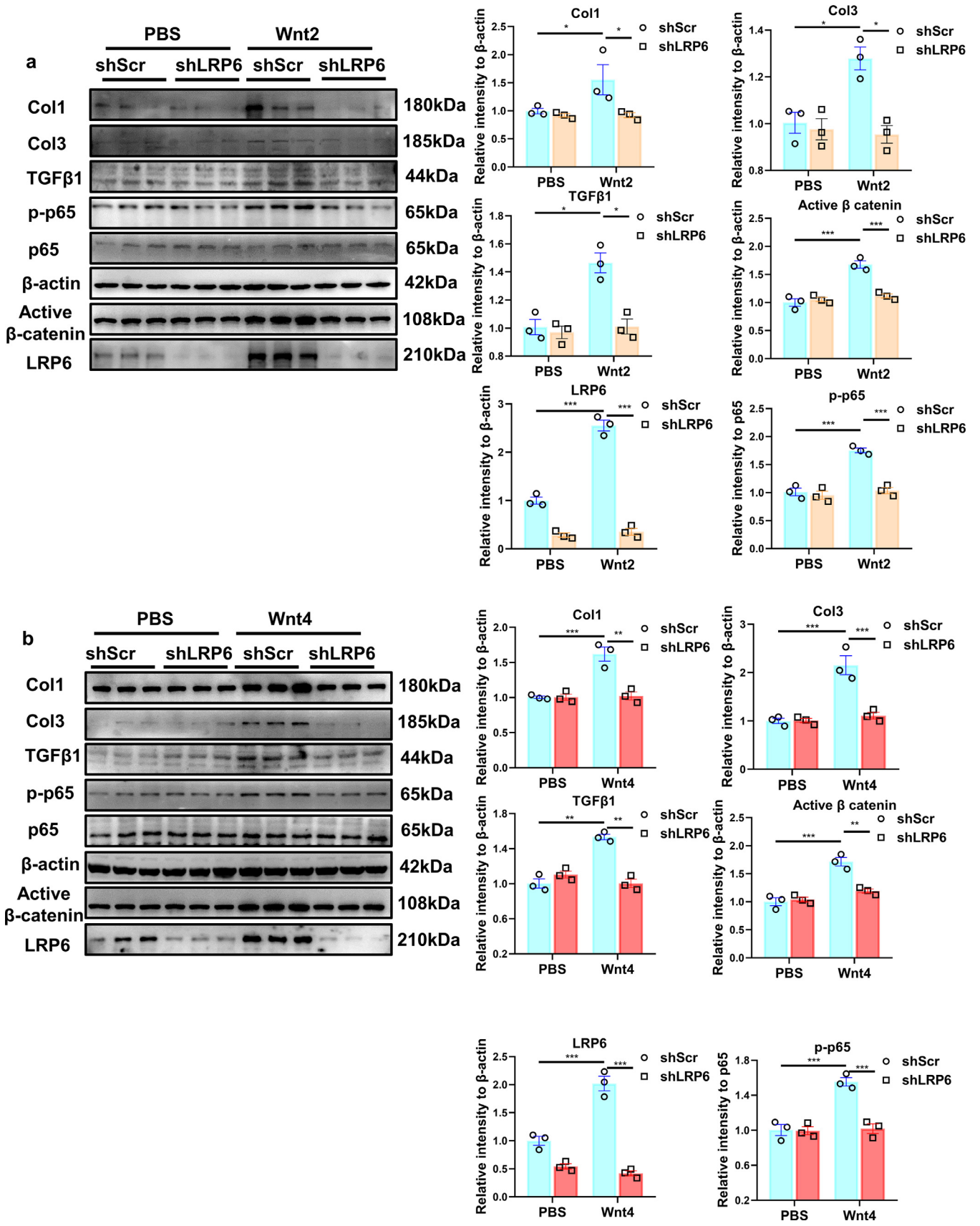
Fig. 5. Wnt2 or Wnt4 activates NF-κB pathway signaling and enhances the expression of Fzd4/Fzd2 in neonatal rat cardiac fibroblasts (NRCFs) in response to hypoxia. (a) The expressions of p-p65, P65, Fzd2 and Fzd4 in NRCFs were detected by Western blot analysis. $n = 4$/group. (b) The expressions of p65 and β-catenin were detected in nucleus of NRCFs by western blot. $n = 3$/group. (a,b) These NRCFs were pretreated with siRNA targeted Wnt2 or Wnt4 (si-Wnt2 or si-Wnt4) or si-Scramble (si-Scram) for 24 h, and then exposed to hypoxia or normoxia (Control) for 3 h. Values were expressed as means±S.E.M. * $p < 0.05$, ** $p < 0.01$, *** $p < 0.001$. (c) The expressions of p-p65, p65, Fzd 2 and Fzd 4 were detected in non-infarcted area by Western blot analysis. 8-10 weeks old male mice were intravenously injected with shWnt2/4-AAV9 (shWnt2/4) or shScramble-AAV9 (shNC) at 3 weeks

Fig. 6. NF-κB inhibitor ameliorates Wnt2/Wnt4-induced pro-fibrotic effects in neonatal rat cardiac fibroblasts (NRCFs). (a,b) The expressions of Col1, Col3, active β-catenin, MMP2, MMP9, p65, p-p65 and TGFβ1 were measured in NRCFs by Western blot analysis. These NRCFs were pretreated with JSH-23(NF-κB inhibitor, 10μM) or the same volume of DMSO for 1 h, followed by PBS, human recombinant Wnt2 (20 ng/ml) or Wnt4 (50 ng/ml) treatment for 24 h. Values were expressed as means±S.E.M. * $p < 0.05$, ** $p < 0.01$, *** $p < 0.001$; n = 3 in each group. Statistics: Two-way ANOVA with a Bonferroni post hoc test.

Fig. 7. Wnt/β-catenin inhibitor relieves Wnt2/Wnt4-induced pro-fibrotic effects in neonatal rat cardiac fibroblasts (NRCFs). (a,b) The expressions of Col1, Col3, active β-catenin, p65, TGFβ1, Fzd2, Fzd4 and p-p65 were measured in NRCFs by Western blot analysis. These NRCFs were pretreated with ICG-001(β-catenin inhibitor, 10 μM) or the same volume of DMSO for 1 h, followed by PBS, human recombinant Wnt2 (20 ng/ml) or Wnt4 (50 ng/ml) treatment for 24 h. Values were expressed as means±S.E.M. * p < 0.05, ** p < 0.01, *** p < 0.001, n = 3 in each group. Statistics: Two-way ANOVA with a Bonferroni post hoc test.

Fig. 8. Knockdown of Fzd2 or Fzd4 attenuates Wnt4- or Wnt2-induced pro-fibrotic effects in neonatal rat cardiac fibroblasts (NRCFs). (a,b) Western blot analysis of the expressions of Fzd2, Col1, Col3, active β-catenin, MMP2, MMP9, TGFβ1, and p-65 in NRCFs. Values were expressed as means±S.E.M. * $p < 0.05$, ** $p < 0.01$, *** $p < 0.001$; n = 3 in each group. Statistics: Two-way ANOVA with a Bonferroni post hoc test. (a) NRCFs were pretreated with siRNA targeted Fzd2 (si- Fzd2) or si-Scramble (si-Scram) for 24 h, followed by PBS, human recombinant Wnt4 (50 ng/ml) treatment for another 24 h. (b) NRCFs were pretreated with siRNA targeted Fzd4 (si- Fzd4) or si-Scramble (si-Scram) for 24 h, followed by PBS, human recombinant Wnt2 (20 ng/ml) treatment for another 24 h.

Fig. 9. Knockdown of LRP6 attenuates Wnt2- or Wnt4-induced pro-fibrotic effects in neonatal rat cardiac fibroblasts (NRCFs). (a,b) Western blot analysis of the expressions of Col1, Col3, active β-catenin, TGFβ1, LRP6 and p-65 in NRCFs. Cultured NRCFs were transfected with lenti-shScr (shScr) or lenti-LRP6(shLRP6) for 48 h and then followed by PBS, human recombinant Wnt2 (20 ng/ml) or Wnt4(50 ng/ml) treatment for another 24 h. Values were expressed as means±S.E.M. * $p < 0.05$, ** $p < 0.01$, *** $p < 0.001$. $n = 3$ /group. Statistics: Two-way ANOVA with a Bonferroni post hoc test.
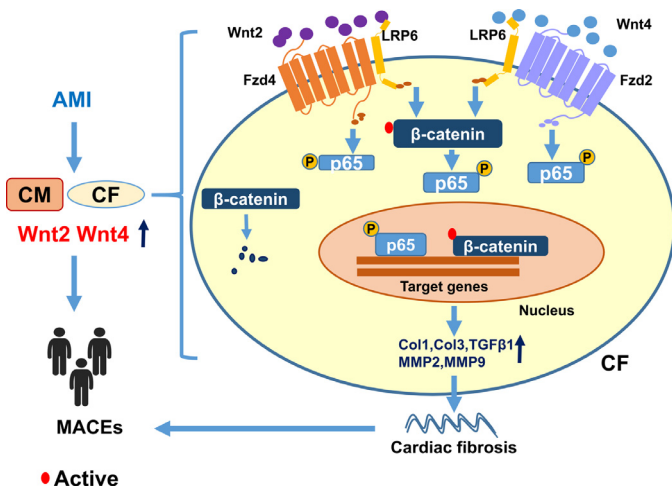
Fig. 10. A proposed model of showing how Wnt2 and Wnt4 promote cardiac fibrosis by activation of β-catenin/NF-κB trough LRP6 and Fzds signaling following MI. MI induced the increased expression or secretion of Wnt2 and Wnt4 in cardiaomyocytes (CMs) or cardiac fibroblasts (CFs), elevated Wnt2 and Wnt4 promote fibrotic effects by activation of β-catenin/NF-κB signaling dependently on the cooperation of Fzd4 or Fzd2 and LRP6 signaling in cardiac fibroblasts, which contributes to cardiac fibrosis and dysfunction post-MI. Thus high Wnt2 and Wnt4 are independently associated with adverse outcome in AMI patients.

function, hypertrophy and fibrosis after experimental MI. *In vitro,* Wnt2 or Wnt4 directly activated fibroblasts but did not show hypertrophic effect on cardiomyocytes, suggesting the pivotal roles of increased Wnt2 and Wnt4 in MI-induced cardiac fibrosis. ShWnt2/4 injection improved cardiac hypertrophy which may be secondary to the decreased cardiac fibrosis following MI. Different kinds of porcupine inhibitor (Wnt secretion inhibitor) have been reported to ameliorate adverse cardiac remodeling, improve ventricular function, and inhibit cardiac fibrosis after experimental myocardial infarction [38−40]. *In vitro,* we observed the similar results from the Wnt-C59, a porcupine inhibitor. The cardiac protection of porcupine inhibitors may be related to inhibition of Wnt2 or Wnt4 signaling after MI. Our study provides direct evidence that Wnt2 or Wnt4 promotes cardiac fibrosis in ischemic hearts. Liu J et al reported that Wnt4 negatively regulates skin myofibroblast transition induced by TGF-β1 [41]. It suggests that the roles of Wnt4 in fibroblasts are organ-specific.

Further analysis revealed that the pro-fibrotic roles of Wnt2 and Wnt4 is dependent on the activation of NF-κB/p65, a critical transcriptional factor, which mediates cardiac remodeling following MI [27]. Upon phosphorylation, P65 is activated and translocated from cytoplasm to nucleus to initiate NF-κB target genes transcription, which is crucial for fibroblast growth and collagen accumulation mediated by AngII or pressure overload [42]. Our data revealed that NF-κB/p65 inhibitor greatly inhibited the pro-fibrotic effects of Wnt2 or Wnt4, and *in vivo,* knockdown of Wnt2/4 significantly attenuated the increased p-p65 level. CTGF, one of profibrotic mediators, is regulated by TGF-β1 via NF-κB/p65 or Smad signaling [43]. But knockdown of Wnt2 or Wnt4 did not affect the increased expression of CTGF under hypoxia. These data suggested that Wnt2 or Wnt4 mediates cardiac fibrosis by activation of NF-κB/p65 independently of CTGF signaling following MI. The similar pro-fibrotic effects of Wnt2 and Wnt4 may be related to high homology about 60% of their amino acid sequence [44].

Wnt ligands are extracellular signaling molecules, which transduce signals and exert their actions through Fzd receptors or the co-receptors LRP5/6. The Wnt/Fzd pathway is involved in regulation of fibroblasts activation [45]. TGF-β-induced pro-fibrotic signaling in part by the Frizzled-8 receptor in lung injury [46]. In Penetrating Crohn's Disease, Wnt2b induces epithelial-mesenchymal transition (EMT) via Fzd4 receptor [47]. Fzd4 and Fzd2 have been found to be

abundant in rat cardiac fibroblasts [48]. Knockdown of Fzd4 or Fzd2 attenuated the activation of NF-κB/p65 and pro-fibrotic effects but did not affect the activation of β-catenin induced by Wnt2 or Wnt4, respectively. In addition to Fzd receptor, Wnt 2 and LRP6 have been found to be co-localized in myofibroblasts [49].

Active β-catenin is involved in cardiac fibrosis after MI [26]. Wnt2 or Wnt4 enhanced the expression of LRP6, and knockdown of LPR6 greatly attenuated the activation of β-catenin and NF-κB, and the pro-fibrotic effects of Wnt2 or Wnt4. These data suggested that Wnt2 or Wnt4 induces the activation of β-catenin which is dependent on LRP6 but not Fzd4- or Fzd2 receptor.

In summary, our findings reveal a previously unidentified mechanism by which Wnt2/4 signaling induces cardiac fibrosis. MI induces the increased expression and secretion of Wnt2 and Wnt4 from heart tissue, the increased Wnt2 and Wnt4 activate β-catenin/NF-κB/p65 through the co-operation of LRP6 and Fzd4/2 receptor, which accelerates cardiac fibrosis following MI. These factors contribute to detrimental effects upon the myocardium by promoting a larger infarct size and cardiac dysfunction. It could explain the positive association between high serum Wnt2 and Wnt4 levels and adverse prognosis of AMI patients in our study. Therefore, the present study provides clinical evidence of possible utility of Wnt2 and Wnt4 as a prognostic biomarker or therapeutic target for cardiac fibrosis post-AMI. The limitation of the study is that we did not detect serum Wnt2 or Wnt4 level in long-term following MI. There is of great significance if the relationship between the serum Wnt2 or Wnt4 level and MACEs in a larger AMP populations is confirmed.

Contributors

CY performed most of the experiments, analyzed the data, and wrote the manuscript. ZY collected blood and information from clinical patients, and performed ELISA analysis. JW performed hemodynamic and echocardiographic analysis. CH and LP, provided the support for experimental model. HD, LZ, LG performed follow-up. XJ provided support for statistical analysis. YanZ, XW, YW, performed Masson staining. PG and XY provided experimental material. YunZ provided experimental material and helpful advice. RH, provided clinical design and analyzed data. HG designed the present study, analyzed the data, wrote and revised the manuscript, provided grant support. CY, ZY, HR and HG have verified the underlying data. All authors have read and approved the final version of the manuscript.

Data sharing statement

All the data during the current study have been shown in manuscript and supplemental materials, and unprocessed data are available from the corresponding author on reasonable request.

Declaration of Competing Interest

The authors declare no conflict of interest.

Acknowledgments

Supplementary materials

Supplementary material associated with this article can be found in the online version at doi:10.1016/j.ebiom.2021.103745.

Reference

[1] Townsend N, Wilson L, Bhatnagar P, Wickramasinghe K, Rayner M, Nichols M. Cardiovascular disease in Europe: epidemiological update 2016. Eur Heart J 2016;37(42):3232–45.

[2] Seropian IM, Toldo S, Van Tassell BW, Abbate A. Anti-inflammatory strategies for ventricular remodeling following ST-segment elevation acute myocardial infarction. J Am Coll Cardiol 2014;63(16):1593–603.

[3] van den Borne SW, Diez J, Blankesteijn WM, Verjans J, Hofstra L, Narula J. Myocardial remodeling after infarction: the role of myofibroblasts. Nat Rev Cardiol 2010;7(1):30–7.

[4] Chistiakov DA, Orekhov AN, Bobryshev YV. The role of cardiac fibroblasts in post-myocardial heart tissue repair. Exp Mol Pathol 2016;101(2):231–40.

[5] Clevers H. Wnt/beta-catenin signaling in development and disease. Cell 2006;127 (3):469–80.

[6] Clevers H, Nusse R. Wnt/β-catenin signaling and disease. Cell 2012;149(6):1192–205.

[7] Cingolani OH. Cardiac hypertrophy and the Wnt/Frizzled pathway. Hypertension 2007;49(3):427–8.

[8] Dawson K, Aflaki M, Nattel S. Role of the Wnt-Frizzled system in cardiac pathophysiology: a rapidly developing, poorly understood area with enormous potential. J Physiol 2013;591(6):1409–32.

[9] Mikels AJ, Nusse R. Purified Wnt5a protein activates or inhibits beta-catenin-TCF signaling depending on receptor context. PLoS Biol 2006;4(4):e115.

[10] Lerner UH, Ohlsson C. The WNT system: background and its role in bone. J Intern Med 2015;277(6):630–49.

[11] Aisagbonhi O, Rai M, Ryzhov S, Atria N, Feoktistov I, Hatzopoulos AK. Experimental myocardial infarction triggers canonical Wnt signaling and endothelial-to-mesenchymal transition. Dis Model Mech 2011;4(4):469–83.

[12] Paik DT, Rai M, Ryzhov S, Sanders LN, Aisagbonhi O, Funke MJ, et al. Wnt10b gain-of-function improves cardiac repair by arteriole formation and attenuation of fibrosis. Circ Res 2015;117(9):804–16.

[13] Zeng G, Awan F, Otruba W, Muller P, Apte U, Tan X, et al. Wnt'er in liver: expression of Wnt and frizzled genes in mouse. Hepatology 2007;45(1):195–204.

[14] Wang H, Gilner JB, Bautch VL, Wang DZ, Wainwright BJ, Kirby SL, et al. Wnt2 coordinates the commitment of mesoderm to hematopoietic, endothelial, and cardiac lineages in embryoid bodies. J Biol Chem 2007;282(1):782–91.

[15] Onizuka T, Yuasa S, Kusumoto D, Shimoji K, Egashira T, Ohno Y, et al. Wnt2 accelerates cardiac myocyte differentiation from ES-cell derived mesodermal cells via non-canonical pathway. J Mol Cell Cardiol 2012;52(3):650–9.

[16] Bayle J, Fitch J, Jacobsen K, Kumar R, Lafyatis R, Lemaire R. Increased expression of Wnt2 and SFRP4 in Tsk mouse skin: role of Wnt signaling in altered dermal fibrillin deposition and systemic sclerosis. J Invest Dermatol 2008;128(4):871–81.

[17] Cai Y, Zhu S, Yang W, Pan M, Wang C, Wu W. Downregulation of β-catenin blocks fibrosis via Wnt2 signaling in human keloid fibroblasts. Tumour Biol 2017;39 (6):1010428317707423.

[18] Kispert A, Vainio S, McMahon AP. Wnt-4 is a mesenchymal signal for epithelial transformation of metanephric mesenchyme in the developing kidney. Development 1998;125(21):4225–34.

[19] He YX, Diao TT, Song SM, Wang CC, Wang Y, Zhou CL, et al. Wnt4 is significantly upregulated during the early phases of cisplatin-induced acute kidney injury. Sci Rep 2018;8(1):10555.

[20] DiRocco DP, Kobayashi A, Taketo MM, McMahon AP, Humphreys BD. Wnt4/β-catenin signaling in medullary kidney myofibroblasts. J Am Soc Nephrol 2013;24 (9):1399–412.

[21] Thygesen K, Alpert JS, Jaffe AS, Chaitman BR, Bax JJ, Morrow DA, et al. Fourth universal definition of myocardial infarction (2018) J Am Coll Cardiol 2018;72 (18):2231–64.

[22] Gao E, Lei YH, Shang X, Huang ZM, Zuo L, Boucher M, et al. A novel and efficient model of coronary artery ligation and myocardial infarction in the mouse. Circ Res. 2010;107(12):1445–53.

[23] Ackers-Johnson M, Li PY, Holmes AP, O'Brien SM, Pavlovic D, Foo RS. A simplified, Langendorff-free method for concomitant isolation of viable cardiac myocytes and nonmyocytes from the adult mouse heart. Circ Res 2016;119(8):909–20.

[24] Chen Z, Li Y, Jiang G, Yang C, Wang Y, Wang X, et al. Knockdown of LRP6 activates Drp1 to inhibit survival of cardiomyocytes during glucose deprivation. Biomed Pharmacother 2018;103:1408–14.

[25] Abraityte A, Vinge LE, Askevold ET, Lekva T, Michelsen AE, Ranheim T, et al. Wnt5a is elevated in heart failure and affects cardiac fibroblast function. J Mol Med 2017;95(7):767–77 (Berl).

[26] Hao H, Li X, Li Q, Lin H, Chen Z, Xie J, et al. FGF23 promotes myocardial fibrosis in mice through activation of β-catenin. Oncotarget 2016;7(40):64649–64.

[27] Ma J, Wei M, Wang Q, Li J, Wang H, Liu W, et al. Deficiency of Capn4 gene inhibits nuclear factor-κB (NF-κB) protein signaling/inflammation and reduces remodeling after myocardial infarction. J Biol Chem 2012;287(33):27480–9.

[28] Brown SD, Twells RC, Hey PJ, Cox RD, Levy ER, Soderman AR, et al. Isolation and characterization of LRP6, a novel member of the low density lipoprotein receptor gene family. Biochem Biophys Res Commun 1998;248(3):879–88.

[29] Talman V, Ruskoaho H. Cardiac fibrosis in myocardial infarction-from repair and remodeling to regeneration. Cell Tissue Res 2016;365(3):563–81.

[30] Looi JL, Edwards C, Armstrong GP, Scott A, Patel H, Hart H, et al. Characteristics and prognostic importance of myocardial fibrosis in patients with dilated cardiomyopathy assessed by contrast-enhanced cardiac magnetic resonance imaging. Clin Med Insights Cardiol 2010;4:129–34.

[31] Aizawa T, Karasawa H, Funayama R, Shirota M, Suzuki T, Maeda S, et al. Cancer-associated fibroblasts secrete Wnt2 to promote cancer progression in colorectal cancer. Cancer Med 2019;8(14):6370–82.

[32] Durham AL, McLaren A, Hayes BP, Caramori G, Clayton CL, Barnes PJ, et al. Regulation of Wnt4 in chronic obstructive pulmonary disease. FASEB J 2013;27 (6):2367–81.

[33] Williams H, Mill CA, Monk BA, Hulin-Curtis S, Johnson JL, George SJ. Wnt2 and WISP-1/CCN4 induce intimal thickening via promotion of smooth muscle cell migration. Arterioscler Thromb Vasc Biol 2016;36(7):1417–24.

[34] Tsaousi A, Williams H, Lyon CA, Taylor V, Swain A, Johnson JL, et al. Wnt4/β-catenin signaling induces VSMC proliferation and is associated with intimal thickening. Circ Res 2011;108(4):427–36.

[35] Bartscherer K, Pelte N, Ingelfinger D, Boutros M. Secretion of Wnt ligands requires Evi, a conserved transmembrane protein. Cell 2006;125(3):523–33.

[36] Gross JC, Zelarayán LC. The mingle-mangle of Wnt signaling and extracellular vesicles: functional implications for heart research. Front Cardiovasc Med 2018;5:10.

[37] Galli LM, Burrus LW. Differential palmit(e)oylation of Wnt1 on C93 and S224 residues has overlapping and distinct consequences. PLoS ONE 2011;6(10):e26636.

[38] Moon J, Zhou H, Zhang LS, Tan W, Liu Y, Zhang S, et al. Blockade to pathological remodeling of infarcted heart tissue using a porcupine antagonist. Proc Natl Acad Sci U S A. 2017;114(7):1649–54.

[39] Bastakoty D, Saraswati S, Joshi P, Atkinson J, Feoktistov I, Liu J, et al. Temporary, systemic inhibition of the WNT/β-catenin pathway promotes regenerative cardiac repair following myocardial infarct. Cell Stem Cells Regen Med 2016;2(2).

[40] Yang D, Fu W, Li L, Xia X, Liao Q, Yue R, et al. Therapeutic effect of a novel Wnt pathway inhibitor on cardiac regeneration after myocardial infarction. Clin Sci 2017;131(24):2919–32 (Lond).

[41] Liu J, Zhao B, Zhu H, Pan Q, Cai M, Bai X, et al. Wnt4 negatively regulates the TGF-β1-induced human dermal fibroblast-to-myofibroblast transition via targeting Smad3 and ERK. Cell Tissue Res 2020;379(3):537–48.

[42] Wei C, Kim IK, Kumar S, Jayasinghe S, Hong N, Castoldi G, et al. NF-κB mediated miR-26a regulation in cardiac fibrosis. J Cell Physiol 2013;228(7):1433–42.

[43] Nagai Y, Matoba K, Kawanami D, Takeda Y, Akamine T, Ishizawa S, et al. ROCK2 regulates TGF-β-induced expression of CTGF and profibrotic genes via NF-κB and cytoskeleton dynamics in mesangial cells. Am J Physiol Renal Physiol 2019;317 (4):F839–f51.

[44] Gavin BJ, McMahon JA, McMahon AP. Expression of multiple novel Wnt-1/int-1-related genes during fetal and adult mouse development. Genes Dev 1990;4 (12b):2319–32.

[45] Laeremans H, Rensen SS, Ottenheijm HC, Smits JF, Blankesteijn WM. Wnt/frizzled signalling modulates the migration and differentiation of immortalized cardiac fibroblasts. Cardiovasc Res 2010;87(3):514–23.

[46] Spanjer AI, Baarsma HA, Oostenbrink LM, Jansen SR, Kuipers CC, Lindner M, et al. TGF-β-induced profibrotic signaling is regulated in part by the WNT receptor Frizzled-8. FASEB J 2016;30(5):1823–35.

[47] Ortiz-Masià D, Salvador P, Macias-Ceja DC, Gisbert-Ferrándiz L, Esplugues JV, Manyé J, et al. WNT2b activates epithelial-mesenchymal transition through FZD4: relevance in penetrating Crohn's disease. J Crohns Colitis 2020;14(2):230–9.

[48] Snead AN, Insel PA. Defining the cellular repertoire of GPCRs identifies a profibrotic role for the most highly expressed receptor, protease-activated receptor 1, in cardiac fibroblasts. FASEB J 2012;26(11):4540–7.

[49] Hughes KR, Sablitzky F, Mahida YR. Expression profiling of Wnt family of genes in normal and inflammatory bowel disease primary human intestinal myofibroblasts and normal human colonic crypt epithelial cells. Inflamm Bowel Dis 2011;17(1):213–20.